exeley INTERNATIONAL JOURNAL ON SMART SENSING AND INTELLIGENT SYSTEMS
Article | DOI: 10.21307/ijssis-2020-005
Issue 1 | Vol. 13 (2020)

LiDAR derived terrain wetness indices to infer soil moisture above underground pipelines

David Bretreger[1], In-Young Yeo[1] and Robert Melchers[1]

[1]School of Engineering, The University of Newcastle, Callaghan, Australia.

E-mails: David.Bretreger@newcastle.edu.au, In-Young.Yeo@newcastle.edu.au and Rob.Melchers@newcastle.edu.au

This paper was edited by Mohamed Serry.

Received for publication December 20, 2019.

Abstract

Corrosion of external cast-iron pipe surfaces, a major contributor to pipe failure, has been attributed to the free water in the soil surrounding the pipe. Because observation at pipe depth is difficult, a potential proxy is the soil surface moisture. Herein highly accurate elevation data derived from airborne light detection and ranging is used to model the distribution of soil water in urban catchments containing pipe infrastructure. The results are compared with local soil moisture Theta Probe measurements along the pipe. The results show potential to identify wetter spots above underground infrastructure, which may inform its corrosion potential, without digging up the asset.

Keywords

Pipe corrosion, Pipe breaks, Topographic wetness index, SAGA wetness index, Infrastructure assessment.

Many major cities such as Sydney have extensive networks of water supply pipelines, including major trunk lines that are ageing and increasingly prone to failure. Many of these pipes are made of cast iron. This material is traditional and has been shown to have excellent long-term durability, with many pipes surviving well past 100 years. Others, however, fail much earlier, and often this is through corrosion of the external surfaces of pipes. Such corrosion usually leads to weakening of pipe walls and eventually to pipe failure (Melchers, 2017). The mechanisms involved have been the subject of an extensive recent research programme (Melchers et al., 2018, 2019; Petersen and Melchers, 2014, 2019). Previous work identified that, apart from workmanship issues associated with the initial installation of the pipes and their burial, a major factor in the corrosion of the pipes at depth, typically one metre but sometimes much more, is the free water that can make its way from the surface through the backfill soil to the pipe exterior walls. The major contributor to this free water is rainfall, and the associated accumulation of water in the soil surrounding the pipe.

Terrain indices are commonly used to map the spatial variability of soil moisture and identify those areas prone to saturation (Kemppinen et al., 2018; Kim, 2009; Tenenbaum et al., 2006; Western et al., 1999). These indices describe the spatial distribution of soil moisture through a catchment based on elevation change (i.e. local slope) and the contributing area. Originally these techniques are used in natural catchments, although they show potential for testing in urban catchments, similar to that described in this work. For example, a topographic wetness index (TWI) (Beven and Kirkby, 1979) has been used successfully to assess the stability of a rail line corridor in the United Kingdom based on the soil moisture distribution (Hardy, 2010). For any assessment with terrain indices, accurate elevation data is required. Airborne light detection and ranging (LiDAR) technology measures return laser pulses, typically from an aircraft. This technique has the ability to estimate distances, and hence elevations, extremely accurately at a high spatial resolution. LiDAR data are commonly used for terrain indices analysis and have been shown to provide accurate results (Kemppinen et al., 2018; Tenenbaum et al., 2006; Hardy, 2010; Thomas et al., 2017; Lang et al., 2012; Vaze and Teng, 2007; Vaze et al., 2010).

The work described herein shows that terrain indices derived from airborne LiDAR can be used to map the spatial variability of soil moisture in the corridors along pipe infrastructure. This will be of assistance in the assessment of corrosion potential of buried infrastructure and aid in mitigating its impacts, both economically for the water authority and for the community.

Methodology

Study area and data

The study area for the present project was limited to a single pipeline. It is located within Jesmond Park, a public park located in Newcastle, NSW, Australia (Figure 1). The pipeline is part of the water supply infrastructure managed by Hunter Water Corporation (HWC), the local water authority. The park is managed by the City of Newcastle and subject to typical management practices and maintenance, including watering. The catchment was selected because it has a mixture of pervious and impervious surfaces, each of which contribute in a different way to surface and subsurface water runoff and routing. This was considered desirable to test the effectiveness of the LiDAR terrain index methodology and also to permit comparison with previous work that involved measurements of corrosion pitting depth (Melchers, 2019).

LiDAR data were provided by HWC for their area of operations. This data set was originally collected by NSW Land and Property Information over NSW (now held by NSW Spatial Services). It was provided in a point-cloud format that allowed different point classifications to be included in the creation of the elevation model. The data set used in this study was collected with a Leica ALS50-II device on 14 September 2014 and was provided with points already classified. The accuracy of the data is 0.3 m

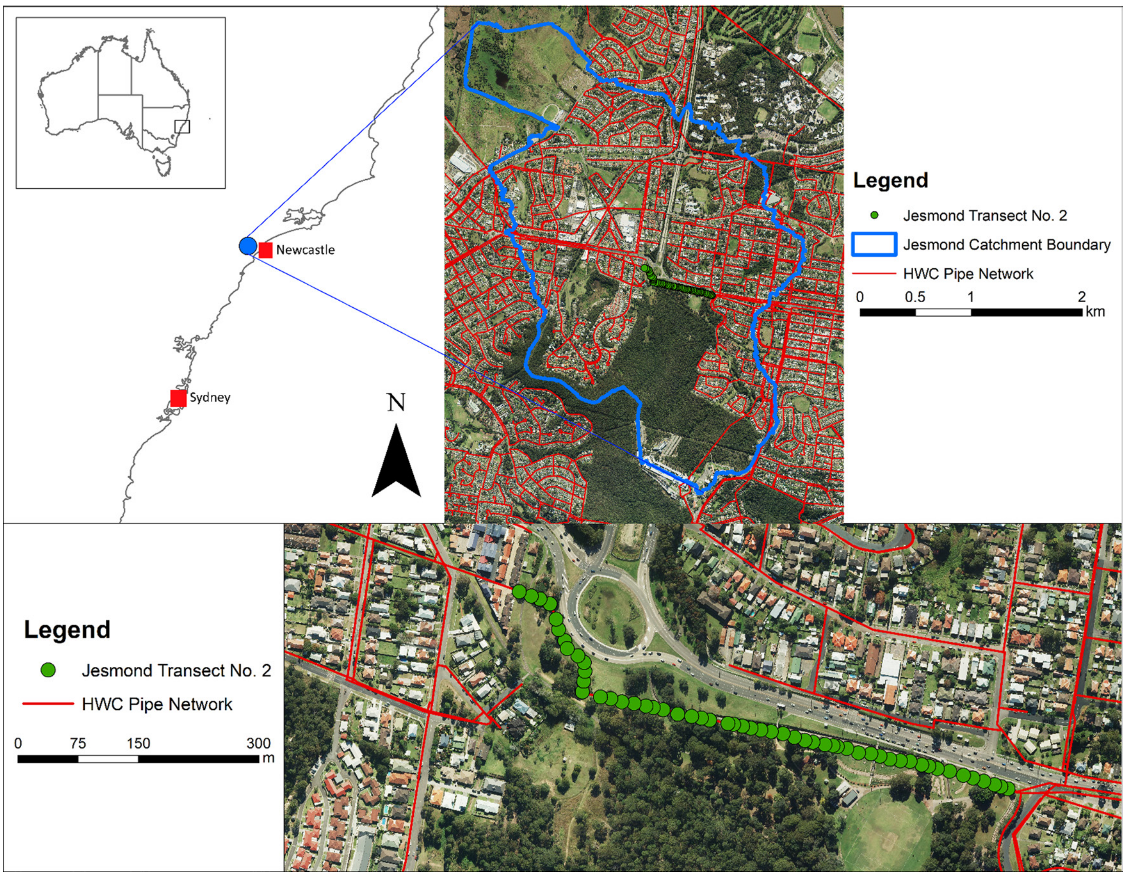

Figure 1: Location of study catchment and example of soil moisture transect.

vertically and 0.8 m horizontally with 95% confidence (Batchelor, 2015).

Terrain index

Terrain indices are used to calculate the accumulation of soil moisture for each cell, into which the catchment of interest has been divided. For a rectilinear regular grid this means that each cell is surrounded by eight neighbouring cells, including those at the corners. The water accumulation is derived from the catchment contributing area and its slope, to obtain the spatial distribution of relative wetness. An important aspect of each terrain index is the flow routing algorithm associated with it since this algorithm calculates the water flow direction based on elevation changes in neighbouring cells.

The terrain index used in the present study is the SAGA wetness index (SWI) (Conrad et al., 2015). According to Lang et al. (2012), this uses the FD8 flow routing algorithm (Freeman, 1991). The FD8 algorithm routes water to all eight neighbouring cells determined by slope, with steeper slopes causing more water to move in that direction. Other algorithms such as D8 or D∞ route to only one or two neighbouring cells (Lang et al., 2012).

The SWI is recommended for use on valley floors as it represents more accurately the lateral redistribution of moisture, at least to compare the TWI (Millard and Richardson, 2014). This might be expected as SWI was designed for use where there are small vertical distances between channels and the base of the valley (Olaya and Conrad, 2009; Boehner et al., 2002). The SWI has been preferred in other studies (Kemppinen et al., 2018). Since the present study is in an urban setting, many of the flow paths are altered from their natural conditions and to better fit those of a valley floor with little difference in vertical elevation between neighbouring cells. The SWI is defined as:

$$SWI = \ln\left(\frac{SCA_m}{\tan(\beta)}\right), \tag{1}$$

where SWI is the SAGA wetness index at a given point, SCA_m is the modified specific catchment area draining to that cell, and β is the slope angle of the point (Boehner and Selige, 2006). Higher values of the SWI represent wetter conditions.

For the present study, the SWI was calculated using the notion that depressions in the (local) topography are not filled with water. This is considered more representative of local-scale elevation depressions (Lang et al., 2012) and how free moisture may accumulate around pipe infrastructure.

LiDAR processing

The LiDAR point cloud data set was processed to remove high and medium vegetation from the data set to create an elevation model that shows minor vegetation noise on the ground as well as urban infrastructure (i.e. houses, buildings and roads). This was done to allow the flow routing of the SWI function to portray realistic flow directions. The point cloud data set was processed using ArcMap v10.6.1 to create an elevation data set with a 1 m resolution over the study catchment. The 1 m resolution was adopted for the present study as it has been reported to provide accurate results for larger-scale topographic indices and hydrologic modelling (Vaze and Teng, 2007; Vaze et al., 2010). The resulting elevations were used to delineate the catchment using functions from SAGA v2.3.2 (Conrad et al., 2015) via the QGIS v3.4.9 long-term release interface. This was done to reduce the number of cells used in computations without removing any that affect the contributing area (i.e. SCA_m) from the SWI calculations. The catchment delineation was completed using a catchment depression filling routine (Wang and Liu, 2006) which fills localised depressions to ensure hydrologically connected contributing upland areas (i.e. SCA_m) are derived. It is important to note, although the catchment was derived using a filled elevation, the unfilled catchment elevation was used for the SWI calculation for a given point, as discussed in the previous section.

Soil moisture data collection

Soil moisture data were collected using a Delta-T Theta Probe (ML3), with a Delta-T HH2 Moisture Meter for reading values (Delta-T Devices Ltd, 2013). The probe can penetrate approximately 6 cm into the soil, and works by measuring the dielectric constant of the soil (Figure 2). More detailed information about the procedure and the measurement technique is available, as reported by Matula et al. (2016). Soil moisture observations were collected on three transects along the specified pipeline. This was to allow various moisture conditions to be observed. At each point, the probe was inserted into the ground at three locations within a $0.5\,m \times 0.5\,m$ quadrat. To account for the localised spatial variability of soil moisture, three readings were taken and then averaged for the comparison with the SWI. The soil moisture transects were completed on 23 August 2019, 5 September 2019 and 24 September 2019.

The location of each sampling point was recorded with a Garmin eTrex H GPS unit for georeferencing

Figure 2: Theta Probe used for soil moisture measurements along the transect.

to compare with the SWI. The location of each measurement along transects 2 is plotted in Figures 1 and 3 (lower).

Results and discussion

The soil moisture readings taken at transects 1, 2 and 3 had average values of 14.25, 30.59 and 31.68%, respectively, with standard deviations 5.56, 10.69 and 9.64%. For transect 1, the average moisture readings are consistent with the occurrence of some minor recent rainfall events but no significant rainfall for many weeks before the soil moisture readings were taken. However, for transects 2 and 3, large storm events occurred in the week leading up to the sampling date. Although the minimum soil moisture content readings remained relatively constant (6.0, 8.1 and 9.0%) the maximum and range varied quite significantly between the transects. The maximum soil moisture of 29.0% in transect 1 compares with 53.7 and 55.0% in transects 2 and 3. The differences in maximum and minimum soil moisture follow a similar pattern, with transects 1, 2 and 3 returning values of 23.0, 45.6 and 46.0%. It should be noted that the transects were to be performed at various times after rain, in order to allow estimation of the changes in moisture conditions and their spatial distributions between sampling dates. In turn, this was done to allow assessment of the effect differing moisture contents and thus the suitability of SWI for predicting soil moisture distributions in various degrees of wetness.

Figure 3 shows the output of the SWI calculations for the catchment area and the observation points for transect number 2. The locations marked in red show depressions with relatively large contributing area, which would be expected to permit more soil moisture accumulation. The point-wise variation demonstrates the spatial variability of wetness identified across the pipeline. Extremely low and negative values are seen at houses and for steep slopes (i.e. high β, see Equation (1)) with small catchment areas (i.e. low SCA_m), indicating these cells have low soil moisture accumulation.

Figure 4 shows the regression equations of the three transects considered herein. The derived

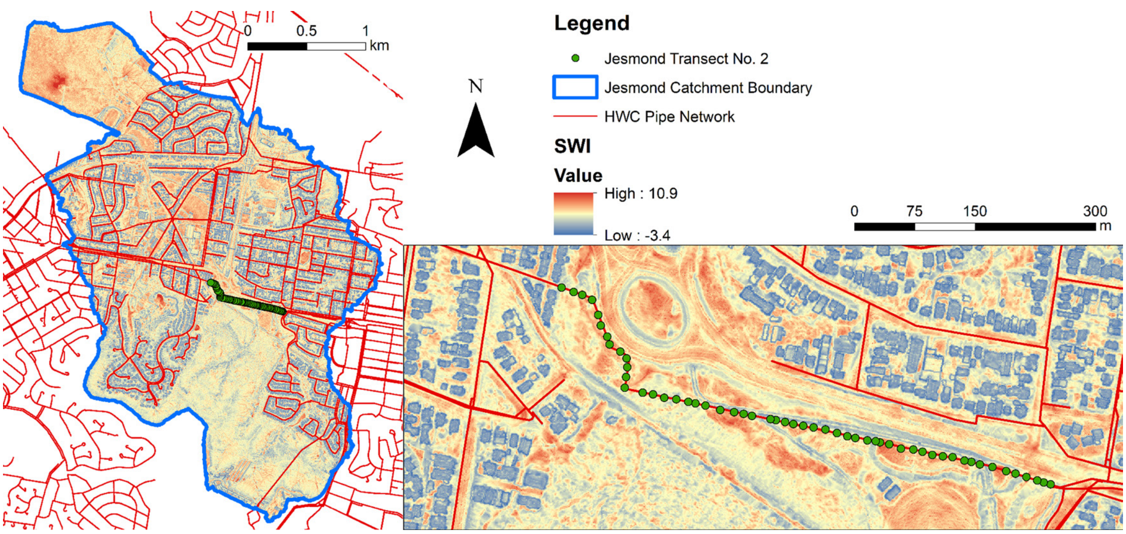

Figure 3: SAGA wetness index (SWI) results over the Jesmond study catchment.

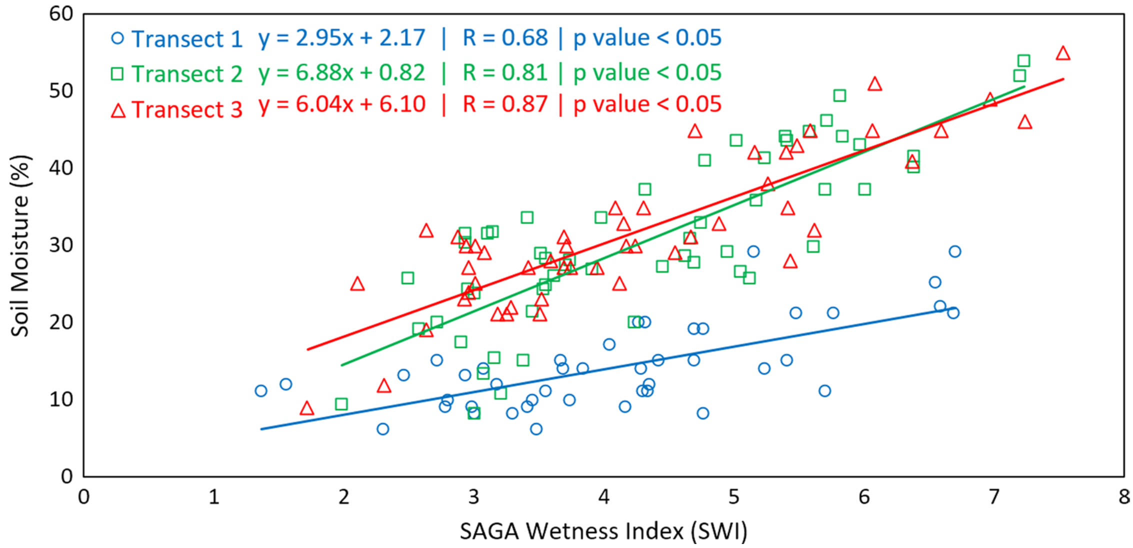

Figure 4: SAGA wetness index (SWI) and soil moisture probe data. The three transects are presented together to show the difference in wetness between the sampling dates.

regression coefficients *R* indicate a reasonable correlation between the SWI and the soil moisture in all conditions. Additionally, each regression equation returned a *p*-value of less than 0.05, indicating all correlations are significant. Better results are seen for transects 2 and 3, when the average soil moisture increases (to 30.59 and 31.68%) leading to an *R* value of 0.81 and 0.87 (p-value < 0.05). This trend agrees with similar results in the literature using terrain indices that observed wetter conditions providing better correlations with soil moisture (Tenenbaum et al., 2006; Western et al., 1999; Hardy, 2010). It is considered likely that the lower accuracy during drier conditions is caused by a continuous lack of rain, and hence very low levels of soil moisture, as well as the drying of soil across horizontal planes, without runoff routing occurring for redistribution of stored soil water (i.e. for transect 1, when the average soil moisture was 14.25% the correlations returned an *R* value of 0.68 (p-value < 0.05). This indicates that the LiDAR-based procedure still provided a reasonable estimation of the soil moisture content and its spatial distribution. Under the dry conditions experienced when observations for transect 1 were performed, the reduced soil moisture range could be responsible for the poorer correlation results (compared to transects 2 and 3), as a smaller range prevents the SWI from establishing the relative moisture as is seen in wetter conditions.

It is likely that in extremely wet conditions the terrain indices will reduce in effectiveness as the spatial distribution of water will show high moisture at all points being assessed. This aspect will need further investigation.

In addition to the work described above using SWI, the standard TWI technique was tested over the three transects using the D8 and D∞ flow routing algorithm. The results from these tests are not presented herein but showed poor relationships with the soil moisture probe measurements. This suggests that for urban environments such as studied herein, SWI may be better suited to soil wetness modelling.

Although the Theta Probe only measures soil moisture 6 cm deep, previous studies indicate that these values are likely to have closely similar mean, variance and frequency distribution to soil moisture values at depths up to 30 cm (Wilson et al., 2003; Bretreger et al., under review). The correlation of the 6 cm soil layer to deeper layers needs further investigation.

As mentioned, the measurement of moisture at pipe depth (around 1 m deep or more) is problematic. However, the 6 cm validation as reported herein may be sufficient to give confidence to inform asset managers of the relative accumulation of soil moisture at practical pipe depths, although further investigation with conditions at greater depth is considered warranted.

Although the SWI is providing a good correlation with soil moisture for the three transects considered herein, it is clearly a relative measure that must be interpreted such as through correlations as shown in Figure 4. Finally, it is important to note that the SWI is a static measure of relative wetness for the specific catchment for which it was determined. As such it cannot be directly used to compare soil moisture in the time domain (i.e. temporally).

Conclusion

The SWI was found to give an indication of the spatial distribution of relative soil moisture around a localised catchment, based on elevation changes, and subsequent runoff and routing flow paths and potential moisture accumulation. The presented results show that SWI is effective in providing trends of soil moisture distribution at up to a 6 cm depths along a pipeline in this catchment. The effectiveness of the SWI based method was reduced when using it in drier conditions. This is likely due to less variability in soil moisture.

The results presented herein provide support for further work to assess the ability of SWI for predicting spatial soil moisture variability and patterns for the localised catchments relevant for underground pipelines and other infrastructure and their condition and corrosion assessment.

Acknowledgments

The authors would like to thank Ian Hiles from Hunter Water Corporation for providing the LiDAR and pipe spatial data. The authors would also like to thank Chun Yu Wong and Ankur Srivastava for their help when collecting the field data used in this paper. Sydney Water Corporation and Hunter Water Corporation supported this work through the NSW Smart Sensing Network's Critical Underground Pipe Sensing project.

Literature Cited

Batchelor, M. 2015. Managing big data in a small office: how can we best utilise LiDAR and Aerial photography. Presented at the 20th Association of Public Authority Surveyors Conference (APAS2015), Coffs Harbour, 16–18 March.

Beven, K. J. and Kirkby, M. J. 1979. A physically based, variable contributing area model of basin hydrology/Un modèle à base physique de zone d'appel variable de l'hydrologie du bassin versant. *Hydrological Sciences Bulletin* 24(1): 43–69.

Boehner, J. and Selige, T. 2006. Spatial prediction of soil attributes using terrain analysis and climate regionalisation. in Boehner, J., McCloy, K. R. and Strobl, J. (Eds), *SAGA – Analysis and Modelling Applications* 115 Goettinger Geographische Abhandlungen, Goettingen, pp. 13–28.

Boehner, J., Kothe, R., Conrad, O., Gross, J., Ringeler, A. and Selige, T. 2002. Soil regionalisation by means of terrain analysis and process parameterisation. Research Report No. 7, European Soil Bureau, Luxembourg, pp. 213–222.

Bretreger, D., Hancock, G., Yeo, I.-Y., Martinez, C., Wells, T., Cox, T., Kunkel, V., Gibson, A. under review. Determining soil moisture using portable probes: a comparison of different methods at the large catchment scale. *Journal of Hydrology*.

Conrad, O., Bechtel, B., Bock, M., Dietrich, H., Fischer, E., Gerlitz, L., Wehberg, J. M., Wichmann, V., Böhner, J. 2015. System for Automated Geoscientific Analyses (SAGA) v. 2.1.4. *Geoscientific Model Development* 8(7): 1991–2007.

Delta-T Devices Ltd 2013. *User Manual for the Moisture Meter type HH2* Delta-T Devices, Cambridge.

Freeman, T. G. 1991. Calculating catchment area with divergent flow based on a regular grid. *Computers & Geosciences* 17(3): 413–422.

Hardy, A. J. 2010. Mapping soil moisture as an indicator of transport corridor slope instability using remotely sensed data. *Journal of Maps* 6(S1): 1–11.

Kemppinen, J., Niittynen, P., Riihimäki, H. and Luoto, M. 2018. Modelling soil moisture in a high-latitude landscape using LiDAR and soil data. *Earth Surface Processes and Landforms* 43(5): 1019–1031.

Kim, S. 2009. Characterization of soil moisture responses on a hillslope to sequential rainfall events during late autumn and spring. *Water Resources Research* 45, W09425, doi: 10.1029/2008WR007239.

Lang, M., McCarty, G., Oesterling, R. and Yeo, I.-Y. 2012. Topographic metrics for improved mapping of forested wetlands. *Wetlands* 33(1): 141–155.

Matula, S., Batkova, K. and Legese, W. L. 2016. Laboratory performance of five selected soil moisture sensors applying factory and own calibration equations for two soil media of different bulk density and salinity levels. *Sensors (Basel)* 16(11): 1912, available at: https://doi.org/10.3390/s16111912

Melchers, R. E. 2017. Post-perforation external corrosion of cast iron pressurised water mains. *Corrosion Engineering, Science and Technology* 52(7): 541–546.

Melchers, R. E. 2019. Corrosion of cast iron water mains – developing models for long-term prediction. presented at the International Corrosion Science and Corrosion Engineering Symposium, Melbourne.

Melchers, R. E., Petersen, R. B. and Wells, T. 2018. The effect of atmospheric precipitation on the corrosion of ferrous metals buried in soils. *Corrosion Engineering, Science and Technology* 54(1): 28–36.

Melchers, R. E., Petersen, R. B. and Wells, T. 2019. Empirical models for long-term localised corrosion of cast iron pipes buried in soils. *Corrosion Engineering, Science and Technology* pp. 1–10.

Millard, K. and Richardson, M. 2014. Wetland mapping with LiDAR derivatives, SAR polarimetric decompositions, and LiDAR–SAR fusion using a random forest classifier. *Canadian Journal of Remote Sensing* 39(4): 290–307.

Olaya, V. and Conrad, O. 2009. Chapter 12 geomorphometry in SAGA. in Hengl, T. and Reuter, H. I. (Eds), *Geomorphometry – Concepts, Software, Applications (Developments in Soil Science)*, pp. 293–308.

Petersen, R. B. and Melchers, R. E. 2014. Long term corrosion of buried cast iron pipes in native soils. presented at the Corrosion & Prevention Conference & Exhibition, Darwin, NT, Australia.

Petersen, R. B. and Melchers, R. E. 2019. Effect of moisture content and compaction on the corrosion of mild steel buried in clay soils. *Corrosion Engineering, Science and Technology* 54(7): 587–600.

Tenenbaum, D. E., Band, L. E., Kenworthy, S. T. and Tague, C. L. 2006. Analysis of soil moisture patterns in forested and suburban catchments in Baltimore, Maryland, using high-resolution photogrammetric and LIDAR digital elevation datasets. *Hydrological Processes* 20(2): 219–240.

Thomas, I. A., Jordan, P., Shine, O., Fenton, O., Mellander, P. E., Dunlop, P., Murphy, P. N. C. 2017. Defining optimal DEM resolutions and point densities for modelling hydrologically sensitive areas in agricultural catchments dominated by microtopography. *International Journal of Applied Earth Observation and Geoinformation* 54: 38–52.

Vaze, J. and Teng, J. 2007. High resolution LiDAR DEM – how good is it? in Oxley, L. and Kulasiri, D. (Eds), *MODSIM 2007 International Congress on Modelling and Simulation* Modelling and Simulation Society of Australia and New Zealand, Christchurch, New Zealand, December, pp. 692–698, ISBN: 978-0-9758400-4-7, available at: www.mssanz.org.au/MODSIM07/papers/12_s27/HighResolution_s27_Vaze_.pdf

Vaze, J., Teng, J. and Spencer, G. 2010. Impact of DEM accuracy and resolution on topographic indices. *Environmental Modelling & Software* 25(10): 1086–1098.

Wang, L. and Liu, H. 2006. An efficient method for identifying and filling surface depressions in digital elevation models for hydrologic analysis and modelling. *International Journal of Geographical Information Science* 20(2): 193–213.

Western, A. W., Grayson, R. B., Blöschl, G., Willgoose, G. R. and McMahon, T. A. 1999. Observed spatial organization of soil moisture and its relation to terrain indices. *Water Resources Research* 35(3): 797–810.

Wilson, D. J., Western, A. W., Grayson, R. B., Berg, A. A., Lear, M. S., Rodell, M., Famiglietti, J. S., Woods, R. A., McMahon, T. A. 2003. Spatial distribution of soil moisture over 6 and 30cm depth, Mahurangi river catchment, New Zealand. *Journal of Hydrology* 276(1-4): 254–274.